

Self-Clusterized Glycines on Single-Walled Carbon Nanotubes for Alcohol Sensing

Hyun Jae Song,[†] Yoonmi Lee,[†] Tao Jiang,[§] Adil-Gerai Kussov,[§] Minbaek Lee,[‡] Seunghun Hong,[‡] Young-Kyun Kwon,^{*,§} and Hee Cheul Choi^{*,†}

Department of Chemistry, Pohang University of Science and Technology, San 31, Hyoja-Dong, Nam-Gu, Pohang, Korea 790-784, School of Physics and NANO Systems Institute, Seoul National University, Seoul, Korea 151-747, and Department of Physics and Applied Physics, University of Massachusetts, Lowell, Massachusetts 01854

Received: September 2, 2007; In Final Form: October 16, 2007

Glycines are spontaneously adsorbed to form into self-assembled nanoclusters on single-walled carbon nanotubes (SWNTs). After formation of glycine nanoclusters on SWNTs, the field effect transistor (FET) devices show selective sensing ability to alcohols, such as isopropyl alcohol (IPA), methanol, and ethanol. Upon the adsorption of alcohol, the glycine-coated SWNT-FET devices exhibit pseudo-metallic transport behaviors, whereas the original and glycine-coated devices display conventional p-type transport characteristics. Computational studies support that the gate field screening effect induced by instantly formed glycine–alcohol pair layers seems to be responsible for the pseudo-metallic transport behavior.

Introduction

Single-walled carbon nanotube field effect transistor (SWNT-FET) has been widely investigated as a nanoelectronic platform device for selective and sensitive chemical and biomolecular sensing.^{1–6} During the sensing, the electrical signal change is accomplished either via direct charge injection from guest molecules into electronic bands of carbon nanotubes or by modulation of a Schottky barrier formed at the junctions of carbon nanotubes and metal electrodes.^{1,4} Regardless of the sensing mechanism, the fundamental requirement for the development of a selective sensor is to immobilize “probe” molecules that bind to guest molecules with high specificity on the device. Although most biomolecules, especially antigens and antibodies, are selectively recognized by their counterparts through highly specific multiple intermolecular interactions, it is rare to define explicit chemical molecules that selectively recognize gas molecules. The lack of specificity frequently results in false signals commencing from nonspecifically adsorbed gas molecules on the device. To date, NO₂ and NH₃ gases have been selectively sensed from the mixed gas environment when these gases are exposed to polyethylimine and Nafion-coated SWNT-FET devices, respectively.⁷

Due to its popularity and importance in industrial and personal health care fields, many studies have been performed to develop sensitive electronic sensors to detect alcohols. Previously reported alcohol sensors are mostly based on metal oxides; for example, electronic devices consisting of thin films of multivalent metal ion-doped SnO₂ and TiO₂.^{8,9} In these cases, sensing is accomplished by measuring electric signal changes upon the adsorption followed by oxidative reactions of alcohol molecules on the surface of sensing materials. Despite the successful achievements of fairly high sensitivity, they still lack selectivity,

especially when alcohols are present in an aqueous environment due to the similarities in their molecular structures of functional groups (hydroxyl group, –OH) and polarities. Here, we report alcohol sensing against water and acetone by using SWNT-FET devices coated with glycines, and the plausible sensing mechanism is discussed.

Experimental Section

Growth of SWNTs. SWNTs were synthesized on thermally oxidized (500 nm SiO₂), highly boron-doped Si (100) wafers by using a thermal chemical vapor deposition (CVD) system. Iron oxide catalyst nanoparticles were directly synthesized on patterned catalyst islands by using hydroxylamine-mediated clustering process.¹⁰ After removing the photoresist layer, the substrates were transferred into a thermal CVD system in which CH₄, H₂, and C₂H₄ gases were supplied at flow rates of 1000, 500, and 20 sccm at 900 °C.

Fabrication of SWNT-FET Devices. Two types of CVD-grown SWNT-FET devices were fabricated: (1) SWNT-FET devices containing a single SWNT channel that show complete depletion of hole carriers and (2) SWNT-FET devices containing multiple SWNTs connected between the source and drain electrodes (called “network” devices). The single-nanotube devices were fabricated to have 5 μm of channel length by using a conventional photolithography process using poly(methyl methacrylate) (MicroChem) for deep UV- or Az7210 (Az-EM) for normal UV-equipped mask aligner with a conventional lift-off step using hot acetone. The network devices were made by using a shadow-mask process by placing a homemade Cr shadow mask directly on top of the sample substrates, which allows ~80 μm of channel lengths.⁴ The device fabrication was finalized by defining the source and drain electrodes with 20-nm-thick Au on 15-nm-thick Cr deposited by thermal evaporation. The number of SWNTs connected between the source and drain electrodes was also controlled by regulating the density of iron catalyst nanoparticles. We also tested with HiPco SWNT-FET devices that were prepared as follows: A SiO₂/Si substrate was first patterned with hydro-

* To whom correspondence should be addressed. E-mail: choihc@postech.edu (experimental part), YoungKyun_Kwon@uml.edu (theoretical part).

[†] Pohang University of Science and Technology.

[‡] Seoul National University.

[§] University of Massachusetts.

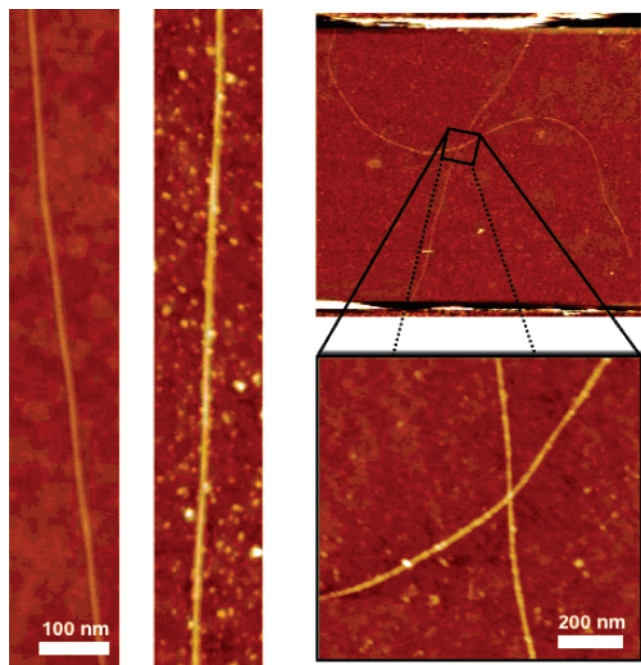


Figure 1. Atomic force microscopy (AFM) images of before (left) and after (center) glycine coating on SWNTs. AFM images of a SWNT-FET device after glycine coating are also shown (right).

phobic octadecyltrichlorosilane, which is designed to prevent the adsorption of SWNTs, by using photolithography and a conventional lift-off process.¹¹ The substrate was then immersed into a 1,2-dichlorobenzene solution containing suspended HiPco-SWNT for 10 s at room temperature. HiPco-SWNTs selectively placed on the polar region of the substrate via van der Waals interactions.

Formation of Glycine Nanoclusters and Electrical Measurements. Glycine nanoclusters were then spontaneously formed on the sidewalls of SWNTs by dispensing several aliquots of aqueous glycine solution (40 mM) onto the channel area of SWNT-FET devices for 1 h at room temperature. The electric transport measurement was performed under ambient conditions by using a semiconductor analyzer (Keithley 4200). Atomic force microscope images were obtained by using a Nanoscope III (Digital Instruments).

Results and Discussion

Glycine, one of the simplest amino acids, is known to have specific interactions with alcohols in biological systems as it protects the liver from alcohol-related injuries by stimulating alcohol metabolism in the stomach.¹² Glycine also involves signal transductions at the nerve synapses as alcohol inhibits the activation of glycine receptors.¹³ Since most of these interactions between glycine and alcohol occur in a biofluidic system that is mainly composed of water, glycine molecules immobilized on a sensor platform are greatly expected to function as a decent probe molecule to screen out alcohols from water.

The average size of glycine nanoclusters spontaneously formed on the sidewalls of SWNTs is ~ 2.5 nm in diameter, and they are hardly removed by a conventional washing process with various solvents (Figures 1 and 2). The nucleation of glycine seems to be initiated by strong nanotube–amine interactions, as previously demonstrated by Smalley et al.¹⁴ and Shim et al.¹⁵ Once a monolayer of glycine is formed, continuous clustering would occur via intermolecular hydrogen bonding interactions among the free glycines and the ones adsorbed on

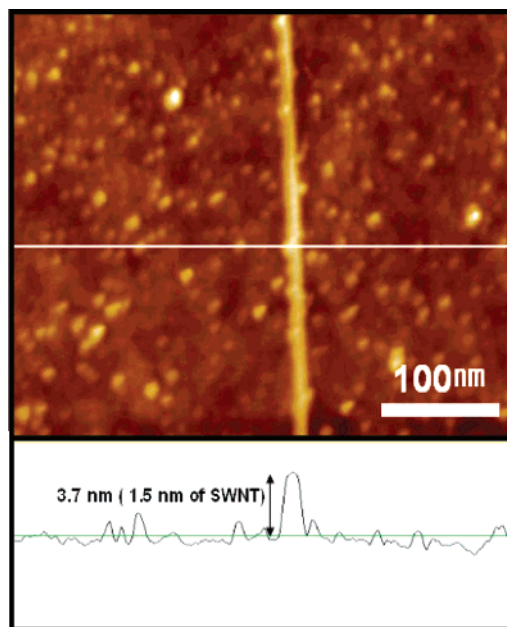


Figure 2. AFM image and height profile of spontaneously formed glycine nanoclusters on a SWNT after vigorous rinsing with DI water and IPA.

SWNTs because glycine contains both a carboxyl and an amine group (Scheme 1). Although glycine nanoclusters are also formed on the surfaces of SiO₂ and metal electrodes through nonspecific bindings, these nanoclusters are not affected on sensing because they are not involved in electrical currents that are mainly flowing through SWNTs.

Specific sensing of alcohol has been investigated by monitoring $I_{DS}-V_G$ characteristic curve changes before and after alcohol adsorption¹⁶ on glycine-coated SWNT-FET devices. As shown in Figure 3, no significant change in transport property has been observed upon the formation of glycine nanoclusters; the glycine-coated SWNT-FET devices still display similar p-type characteristics. This implies that the adsorption of glycine itself does not have any effect on the original charge carrier density in SWNTs, which is verified by our theoretical study described below. However, the $I_{DS}-V_G$ curves of glycine-coated SWNT-FET devices have been dramatically changed upon the adsorption of isopropyl alcohol (IPA), ethanol, and methanol because they show pseudo-metallic behaviors (Figure 4, red curves); i.e., almost no gate dependence upon the gate voltage sweep between -10 and $+10$ V. After testing 10 devices, the relative current variation [$\Delta(I_{DS, \text{sensing}})/\Delta(I_{DS, \text{original}})$] is $\sim 45\%$ for single-channel devices that show complete carrier depletion and $\sim 40\%$ for network devices. Note that $\Delta(I_{DS})$ values are calculated by subtracting the current values measured at the gate voltage of -10 V from the ones measured at the gate voltage of $+10$ V [$\Delta(I_{DS}) = I_{DS}(\text{at } -10 \text{ V}) - I_{DS}(\text{at } +10 \text{ V})$]. Such an obvious and dramatic current variation has been repeated more than 10 times with similar degrees of on/off ratio changes.

The $I_{DS}-V_G$ curve gradually returns to the original shape when the sample is kept in ambient conditions overnight owing to the spontaneous desorption of alcohols from the devices, which signifies that alcohol molecules are not covalently coupled, but weakly physisorbed on the glycine-coated device (Figure 4, green curves). As shown in Figure 5, a time-dependent desorption study indicates that most of the alcohol molecules are desorbed in 6 h. Although the spontaneous desorption of alcohol is highly beneficial in terms of regeneration of sensors, the slow desorption rate is a critical drawback for practical

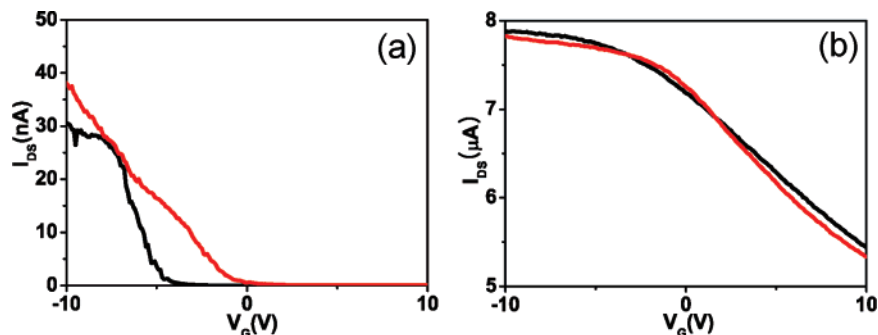


Figure 3. The $I_{DS}-V_G$ characteristic curves of (a) a single-channel SWNT-FET device and (b) a network SWNT-FET device. Black and red curves indicate before and after the formation of glycine nanoclusters, respectively.

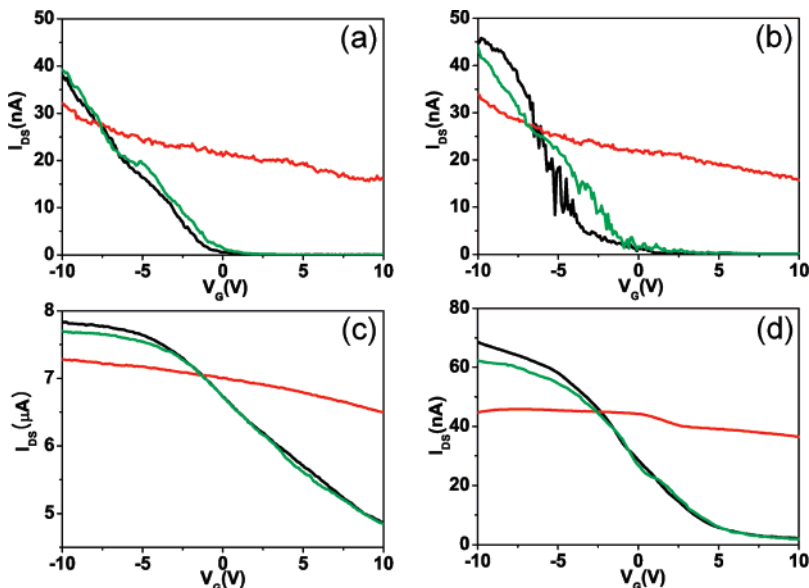
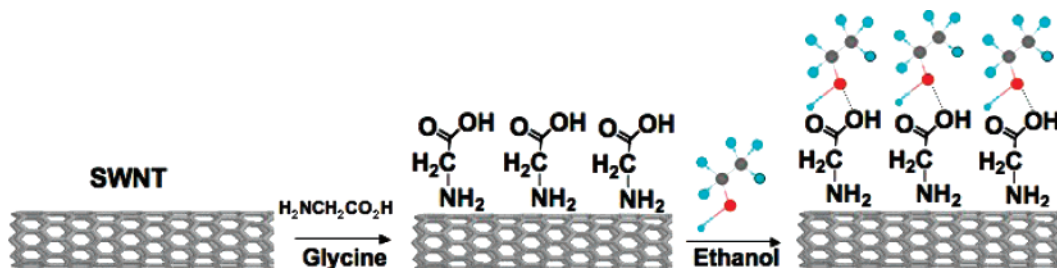


Figure 4. $I_{DS}-V_G$ characteristic curve changes upon alcohol sensing: (a) IPA and (b) ethanol using single-channel SWNT-FET devices and (c) methanol and (d) IPA using network SWNT-FET devices. Black, red, and green curves are obtained after glycine coating, after adsorption of alcohol, and after overnight exposure in air, respectively ($V_{DS} = 10$ mV).

SCHEME 1: A Schematic View of Spontaneous Adsorption of Glycines on SWNT through Nanotube–Amine Interactions and Specific Interaction of Glycines to Alcohols via Hydrogen Bonding Interactions



applications. We have found that desorption of alcohol can be accelerated by either Ar-blowing or heating at low temperature (<100 °C). Especially, an instant recovery of the $I_{DS}-V_G$ curve to its original shape has been achieved upon rinsing the alcohol-adsorbed devices with deionized (DI) water (Figure 6).

Such dramatic changes in $I_{DS}-V_G$ are versatile, regardless of the types of devices. Similar tendencies in the relative current variation have been observed from network devices that have been fabricated using CVD-grown, high-yield SWNTs as well as commercially available HiPco SWNTs. Both devices exhibit a similar trend in $I_{DS}-V_G$ curve changes upon the IPA adsorption on glycine-coated devices (Figure 4c and d for the CVD-grown network devices and Figure 7 for the HiPco network device).

Whereas the glycine-coated SWNT-FET devices show dramatic changes of their transport properties upon alcohol

adsorption, no $I_{DS}-V_G$ curve change has been observed when water or acetone molecules are adsorbed. This implies that acetone and water molecules do not efficiently interact with glycine molecules. To elucidate such discriminating interactions, we have calculated the binding properties of several pairs, such as glycine–IPA (GI), glycine–methanol (GM), glycine–ethanol (GE), glycine–water (GW), and glycine–acetone (GA) near the carbon nanotube by using ab initio density functional formalism^{17–19} based on the pseudopotential method.^{20,21} The wavefunctions have been expanded on a linear combination of atomic orbitals.^{22–25} Exchange–correlation of electrons has been treated with the generalized gradient approximation (GGA) of Perdew, Burke, and Ernzerhof,²⁶ which is believed to be better than the local density approximation²⁷ in describing molecular binding properties. Atomic orbitals with double- ζ polarization

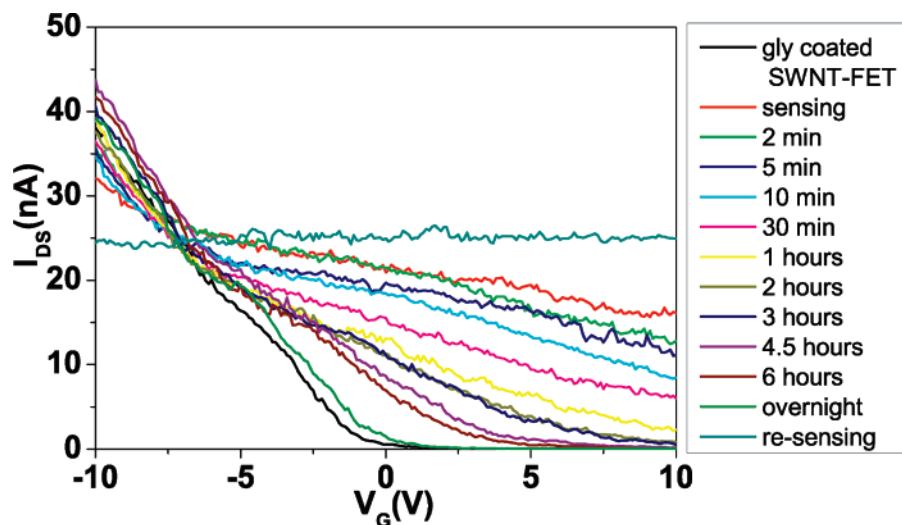


Figure 5. Time-dependent desorption of IPA from a glycine-coated SWNT-FET device in air at room temperature.

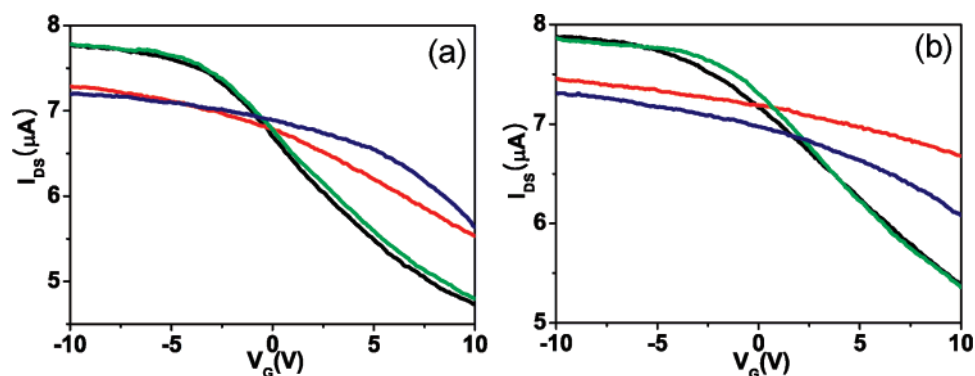


Figure 6. Instant recovery of the glycine-coated SWNT-FET sensors after sensing (a) IPA and (b) ethanol by rinsing with water. I_{DS} - V_G characteristic curves of glycine-coated SWNT-FET device (black), after first sensing with alcohols (red), after rinsing with deionized water followed by N_2 drying (green), after second sensing with alcohols (blue) are shown.

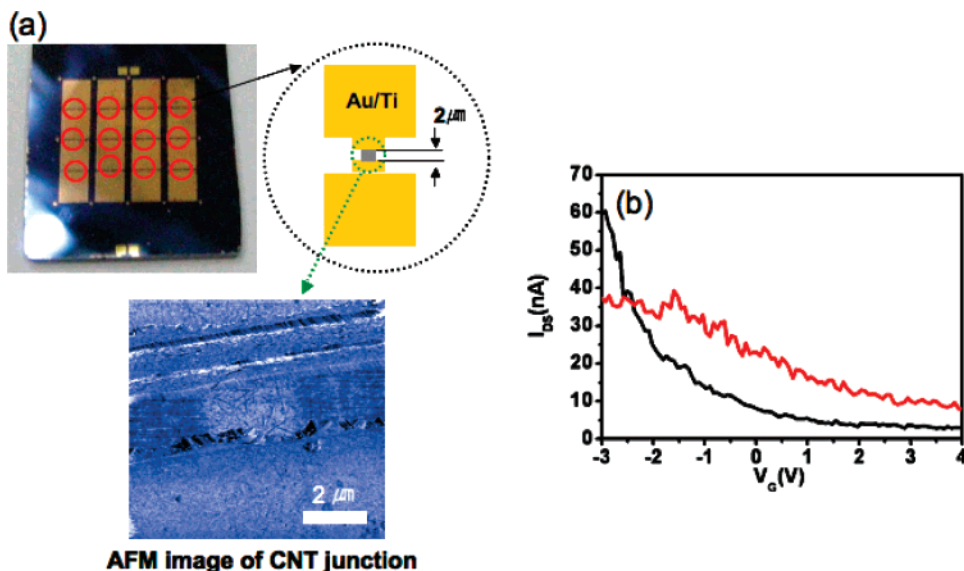


Figure 7. (a) Optical and AFM images of microfabricated HiPco-SWNT-FET devices. (b) I_{DS} - V_G characteristic curves of a glycine-coated HiPco-SWNT-FET device (black) and after sensing with IPA (red) ($V_{DS} = 0.8$ V).

are used to expand single-particle wave functions²³ with the cutoff energy of 150 Ry for real space mesh. We have used 0.01 Ry of the confinement energy shift, which defines the cutoff radii of the atomic orbitals.

Figure 8 displays electron densities of glycine-coated (10, 0) CNT contributed within a few bands near the Fermi level on three slices, showing only very small charge overlap between

two species, from which almost no change is expected in the I_{DS} - V_G , as seen in Figure 3. Relative binding energies between various pairs (GI, GM, GE, GW, and GA) have been calculated using the difference between the total energy of a pair and the sum of the total energies of two individual objects in the pair in the presence of a carbon nanotube. Full relaxations of atomic positions have been carried out to calculate the total energy until

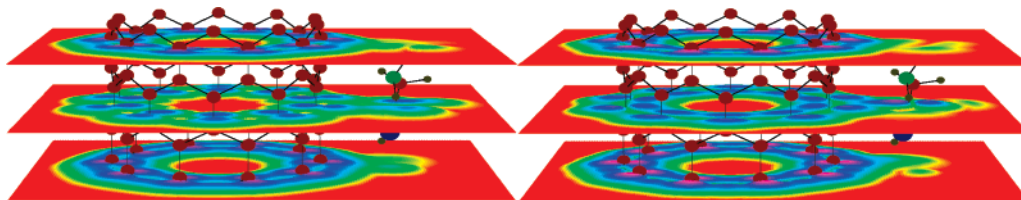


Figure 8. Display of electron densities of glycine-coated (10, 0) CNT contributed from a few bands below and above the Fermi level on three slices. Although glycine and CNTs have relatively strong binding, the charge transfer between the two objects is negligible, confirming our experimental observation of little change in transport behaviors of glycine-coated CNT devices from those of uncoated devices, as shown in Figure 3.

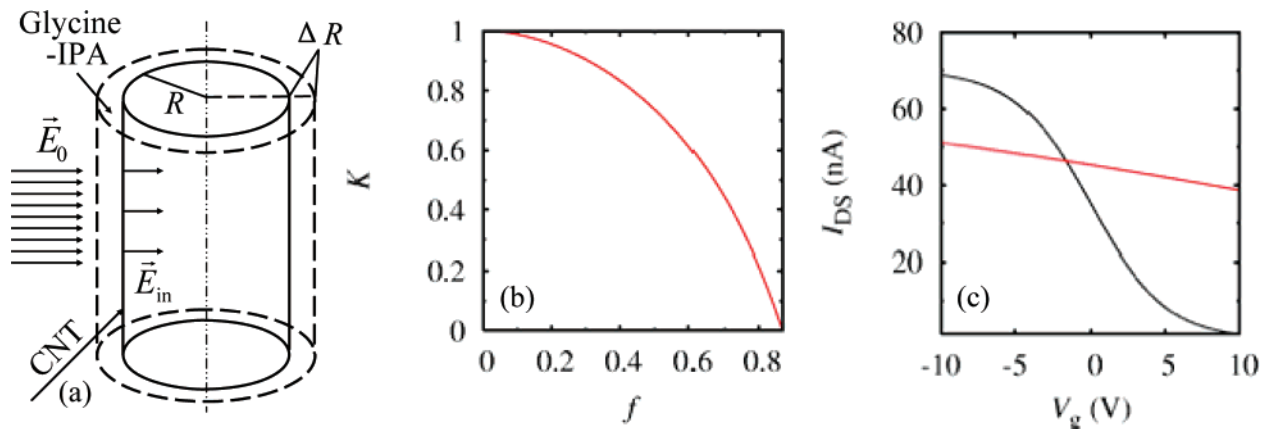


Figure 9. (a) Schematic describing our model for a CNT covered with a glycine–IPA layer (see the text for more information). (b) Screening factor as a function of filling factor. (c) A typical p-type semiconducting I_{DS} – V_G characteristic curve (black) and after forming a cylindrical dipole layer of glycine–alcohol pairs on a SWNT (red) using $K = 0.1$ obtained from $f = 83\%$.

their Hellmann–Feynman forces are less than $0.001 \text{ Ry}/a_B$, with a_B being the Bohr radius. The calculation results show that glycine binds to alcohol with its binding energy of $\sim 0.6 \text{ eV}$ almost independent of alcohol species. It turned out that the difference is only less than a few millielectron volts. The binding of a glycine–alcohol pair is stronger than the binding of GW and GA pairs by ~ 0.28 and $\sim 0.35 \text{ eV}$, respectively. This means that alcohol molecules would be adsorbed or trapped by glycine nanoclusters, although they are not chemically bound, and give a stable sensing state at ambient conditions, whereas water or acetone molecules would desorb relatively easily when their partial pressure is quite low ($< 0.01 \text{ atm}$) according to the van't Hoff equation, leaving glycine-coated nanotubes unchanged, which is in good agreement with our experiments.

In previous studies, the modulation of transport properties of SWNT-FETs upon the adsorption of chemical or biochemical species has been primarily explained by either the charge carrier doping effect or the Schottky barrier modulation effect.^{5,28} The former mechanism involves direct charge (electron or hole) injections into the conduction or valence bands, respectively, upon the adsorption of chemical species. When this happens, obvious shifts of threshold voltage (V_{th}) to either more negative or positive voltages should be observed from I_{DS} – V_G curves, depending on the polarity of the injected charges. In contrast, a similar current change phenomenon is also observable when specific molecular recognition occurs on the Schottky contact region, from which the work function of contact metal is supposed to be modulated. In this case, no V_{th} shift or I_{on} – I_{off} change (upon the gate voltage sweep from -10 to $+10 \text{ V}$) is expected.

None of these mechanisms explains our current results well; i.e., the dramatic and instant changes of p-type characteristic I_{DS} – V_G curves to pseudo-metallic ones. One possible and acceptable rationalization is to suspect if the alcohol layers covering SWNT channels may screen the electric field supplied from a back gate through a SiO_2 dielectric layer. It should be

noted that the adsorbed alcohols cover not only the top surface but also most of the circumferences of SWNTs, as well as the surface of underneath SiO_2 contacting with SWNTs. A similar physisorbed molecule-mediated gate response change phenomenon has been reported by Kim et al.,²⁹ in which physisorbed water molecules around the nanotube circumference turn out to modulate the amounts of trapped charges, which eventually induce significant changes in the I_{DS} – V_G curve shapes (hysteresis).

Therefore, we further investigated the change of the electric field screening factor (K), possibly caused by alcohol molecules wrapping the surface of glycine-coated SWNTs. We have modeled the SWNT covered by glycine–alcohol (GI, GM, or GE) pairs as a cylinder of radius R (SWNT) surrounded by a cylindrical dielectric layer containing dipoles, whose thickness is ΔR , as described in Figure 9a. Then, we have solved the Laplace equation of this model system in the presence of a uniform external electric field, E_0 . The screening factor, K , defined by the ratio of the electric field inside the cylinder, E_{in} , to E_0 , or $K = E_{in}/E_0$, is given by

$$K = \frac{4\epsilon}{(\epsilon + 1)^2 - (\epsilon - 1)^2 \left(\frac{R}{R + \Delta R} \right)^2}$$

which depends on ϵ and ΔR . The permittivity ϵ has been calculated from the Langevin–Debye theory,³⁰ according to which the electrical permittivity, ϵ , is given as a function of microscopic (molecular) polarizability, α ; the dipole moment, p , of the molecular pair; and the filling factor, f (% content of a complex). The resulting formula is

$$\frac{\epsilon - 1}{\epsilon + 2} = f n_0 \left(\frac{4\pi}{3} \right) \alpha + \frac{4\pi}{9} \frac{p^2}{k_B T}$$

where n_0 is the (maximum) ideal number density of GI complexes, estimated to be $n_0 = 3 \times 10^{21} \text{ cm}^{-3}$, and k_B is the Boltzmann constant. α and p of GI pairs are calculated to be 24.2 \AA^3 , and 1.8 Debye, respectively, using our ab initio method. Those values of GM and GE pairs are very similar to the GI pair value mentioned above. f was estimated to be in the range between 50 and 90% from our experimental images (e.g., see Figure 2). At $T = 300 \text{ K}$, $(\epsilon-1)/(\epsilon+2)$ is estimated to be $1.15f$.

The screening factor, K , is calculated as a function of f using $R = 1.5 \text{ nm}$ and $\Delta R = 0.5 \text{ nm}$ and shown in Figure 9b. We apply the screening factor $K = 0.1$ estimated from $f = 83\%$ to a typical $I_{DS}-V_G$ characteristic curve to obtain the corresponding curve after alcohol adsorption. It should be noted that the resulting curve (Figure 9c) looks very similar to those measured experimentally. Not only do water and acetone molecules bind more weakly than alcohol molecules to glycine but also form much weaker dipole moments (one to several orders smaller than that of the GI pair) when they bind to glycine. This is another verification of the alcohol selectivity of glycine-coated nanotube devices over water and acetone.

In conclusion, glycine nanoclusters have been spontaneously formed on the sidewalls of SWNTs, and the glycine-coated SWNT-FET devices show a selective sensing property to alcohols over water and acetone. Prolonged holding of alcohol molecules on glycine-coated SWNTs screens the applied electric gate field, which instantly modulates the conventional p-type transport behavior to a metallic-like one.

Acknowledgment. The author express thanks for support from the Nano/Bio Science & Technology Program of MOST (2006-00955), SRC/ERC Program (R11-2000-070-070020), Korean Research Foundation (MOEHRD, KRF-2005-005-J13103), and KOSEF (2007-8-1158). T.J., A.K., and Y.K. acknowledge support in part from UML Nanomanufacturing Center of Excellence and NSF NSEC: Center for High-Rate Nanomanufacturing, and the computational resources of the National Energy Research Scientific Computing Center, which is supported by the Office of Science of the U.S. Department of Energy under Contract No. DE-AC02-05CH11231. S.H. acknowledges support from the TND program of KOSEF and from MOCIE.

References and Notes

- (1) Kong, J.; Franklin, N. R.; Zhou, C.; Hapline, M. G.; Peng, S.; Cho, K.; Dai, H. *Science* **2000**, *287*, 622–625.
- (2) Someya, T.; Small, J.; Kim, P.; Nuckolls, C.; Yardley, J. *Nano Lett.* **2003**, *3*, 877–881.
- (3) Snow, E. S.; Perkins, F. K.; Houser, E. J.; Badescu, T. L.; Reinecke, T. L. *Science* **2005**, *307*, 1942–1945.
- (4) Byon, H. R.; Choi, H. C. *J. Am. Chem. Soc.* **2006**, *128*, 2188–2189.
- (5) Chen, R.; Choi, H. C.; Bansaruntip, S.; Yenilmez, E.; Tang, X.; Wang, Q.; Chang, Y.-L.; Dai, H. *J. Am. Chem. Soc.* **2004**, *126*, 1563–1568.
- (6) Collins, P. G.; Bradley, K.; Ishigami, M.; Zettl, A. *Science* **2000**, *287*, 1801–1804.
- (7) Qi, P.; Vermesh, O.; Grecu, M.; Javey, A.; Wang, Q.; Dai, H.; Peng, S.; Cho, K. *Nano Lett.* **2003**, *3*, 347–351.
- (8) Yamazoe, N. *Sens. Actuators, B* **1991**, *5*, 7–19.
- (9) Garzella, C.; Comini, E.; Bontempi, E.; Depero, L. E.; Frigeri, C.; Sberveglieri, G. *Sens. Actuators, B* **2002**, *83*, 230–237.
- (10) Choi, H. C.; Kundaria, S.; Wang, D. W.; Javey, A.; Wang, Q.; Rolandi, M.; Dai, H. *Nano Lett.* **2003**, *3*, 157–161.
- (11) Lee, M.; Im, J.; Lee, B. Y.; Myung, M.; Kang, J.; Huang, L.; Kwon, Y.-K.; Hong, H. *Nat. Nanotechnol.* **2006**, *1*, 66–71.
- (12) Iimuro, Y.; Bradford, B. U.; Forman, D. T.; Thurman, R. G. *Gastroenterology* **1996**, *110*, 1536–1542.
- (13) Tao, L.; Ye, J. H. *Br. J. Pharmacol.* **2002**, *136*, 629–635.
- (14) Liu, J.; Casavant, M. J.; Cox, M.; Walters, D. A.; Boul, P.; Lu, W.; Rimberg, A. J.; Smith, K. A.; Colbert, D. T.; Smalley, R. E. *Chem. Phys. Lett.* **1999**, *303*, 125–129.
- (15) Shim, M.; Wong Shi Kam, N.; Chen, R. J.; Li, Y.; Dai, H. *Nano Lett.* **2002**, *2*, 285–288.
- (16) Adsorption of alcohol is conducted as the device is rinsed with alcohols of interest followed by complete drying under a N_2 stream.
- (17) Kohn, W.; Sham, L. *J. Phys. Rev.* **1965**, *140*, A1133–A1138.
- (18) Ihm, J.; Zunger, A.; Cohen, L. M. *J. Phys. C: Solid State Phys.* **1979**, *12*, 4409–4422.
- (19) Payne, M. C.; Teter, M. P.; Allan, D. C.; Arias, T. A.; Joannopoulos, J. D. *Rev. Mod. Phys.* **1992**, *64*, 1045–1097.
- (20) Cohen, L. M. *Phys. Scr.* **1982**, *T1*, 5–10.
- (21) Kleinman, L.; Bylander, D. M. *Phys. Rev. Lett.* **1982**, *48*, 1425–1428.
- (22) Troullier, N.; Martins, J. L. *Phys. Rev. B: Condens. Matter Mater. Phys.* **1991**, *43*, 1993–2006.
- (23) Sanchez-Portal, D.; Ordejon, P.; Artacho, E.; Soler, J. M. *Int. J. Quantum Chem.* **1997**, *65*, 453–461.
- (24) Artacho, E.; Sanchez-Portal, D.; Ordejon, P.; Garcia, A.; Soler, J. M. *Phys. Status Solidi B* **1999**, *215*, 809–817.
- (25) Ordejon, P. *Phys. Status Solidi B* **2000**, *217*, 335–356.
- (26) Perdew, J. P.; Burke, K.; Ernzerhof, M. *Phys. Rev. Lett.* **1996**, *77*, 3865–3868.
- (27) Ceperly, D. M.; Alder, B. J. *Phys. Rev. Lett.* **1980**, *45*, 566–569.
- (28) Radosavljevic, M.; Appenzeller, J.; Knoch, J.; Avouris, Ph. *Appl. Phys. Lett.* **2004**, *84*, 3693–3695.
- (29) Kim, W.; Javey, A.; Vermesh, O.; Wang, Q.; Li, Y.; Dai, H. *Nano Lett.* **2003**, *3*, 193–198.
- (30) Vanderlinde, J. *Classical Electromagnetic Theory*; Springer: New York, 2005; p 175.